Analytical Methods

Cite this: *Anal. Methods*, 2011, **3**, 927

www.rsc.org/methods

PAPER

Voltammetric methods for the speciation of dissolved iron and determination of Fe-containing nanoparticles in mine-water discharge

L. K. Mudashiru,[a] A. C. Aplin[b] and B. R. Horrocks*[a]

Received 11th November 2010, Accepted 28th January 2011
DOI: 10.1039/c0ay00688b

A voltammetric procedure for the determination of total, dissolved, solid phase and nanoparticulate Fe in polluted mine-waters has been developed. Mine-water samples were collected from abandoned mine sites in the UK, which have been designated by the UK Coal Authority for remediation research and for routine monitoring of mine-water quality. Monthly samples were taken over the period March, 2006 to April, 2007 from six different sites in North East England. The samples were analysed directly using differential pulse voltammetry at gold electrodes: separate peaks due to unhydrolysed and hydrolysed Fe aquo ions could be assigned and quantified. The results show that our analysis provides data for total dissolved iron of comparable analytical quality to the established mine-water analysis techniques based on inductively-coupled plasma-optical emission spectroscopy. Further, the difference between differential pulse voltammetry data in acidified and unacidified samples allows quantitation of the Fe-containing solid phase and nanoparticulate Fe oxyhydroxide phases. If samples were pre-filtered, then these measurements also allowed us to determine the fraction of Fe present in nanoparticles <450 nm diameter. Finally, steady-state voltammetry at Pt microelectrodes was used to obtain the ratio of Fe(II) and Fe(III) redox states in the soluble Fe fraction.

1. Introduction

Acidic, metalliferous pollution arising from abandoned mine workings and spoil heaps is a major environmental threat to substantial lengths of river courses worldwide.[1,2] Iron is a key contaminant in mine-waters, occuring in concentrations up to ~0.1 mol dm^{-3} as a result of a series of well-known acidification reactions ultimately related to the oxidation of pyrite (FeS_2) by oxygenated waters penetrating spoil heaps and mine voids. The relevant redox chemistry is summarised in eqn (1)–(4):[3]

$$FeS_2(s) + \frac{7}{2}O_2 + H_2O \rightarrow Fe^{2+} + 2SO_4^{2-} + 2H^+ \quad (1)$$

$$Fe^{2+} + \frac{1}{4}O_2 + H^+ \rightarrow Fe^{3+} + \frac{1}{2}H_2O \quad (2)$$

$$FeS_2(s) + 14Fe^{3+} + 8H_2O \rightarrow 15Fe^{2+} + 2SO_4^{2-} + 16H^+ \quad (3)$$

$$Fe^{3+} + 3H_2O \rightarrow Fe(OH)_3(s)\{ochre\} + 3H^+ \quad (4)$$

The direct reaction of dioxygen with pyrite (eqn (1)) is slow, but iron-oxidizing bacteria can accelerate the oxidation of the Fe^{2+} and facilitate the oxidation of pyrite by Fe^{3+} (eqn (3)), which is rapid and produces a low pH.[3] Mixing of acidic, iron-rich waters with oxygenated, higher pH surface waters results in a series of hydrolysis and oxidation reactions leading to the precipitation of yellow Fe(III) oxyhydroxides called ochre. The presence of iron in mine-waters causes major environmental degradation in surface waters due to the deposition of iron oxides and oxyhydroxides on sub-aqueous plants and river beds.

The abundance of iron in mine-affected waters is generally measured by spectroscopic methods such as atomic absorption spectroscopy or inductively-coupled plasma-optical emission spectroscopy (ICP-OES). Either total iron may be determined, or the waters are filtered at 0.45 μm or 0.2 μm in order to differentiate solid phase and "dissolved" iron. These conventional datasets have two main limitations: they give no idea of the redox state or speciation of iron and do not differentiate colloidal iron (*i.e.*, sub 0.45 μm or 0.2 μm particles) from truly dissolved iron. Ultrafiltration has been used to fractionate colloidal and "dissolved" (<1 kDa) metal-containing species and the results obtained suggest that much of the iron in the sub 0.45 μm filtrate from both uncontaminated and mine-affected water courses is in fact colloidal.[4–10] The environmental significance of colloidal iron is that it (a) absorbs trace metals;[11] (b) is prone to flocculation;[12] and (c) may be less bioavailable than truly dissolved iron.[13]

[a]*School of Chemistry, Bedson Building, Newcastle University, Newcastle Upon Tyne, NE1 7RU, UK. E-mail: b.r.horrocks@ncl.ac.uk*
[b]*School of Civil Engineering & Geosciences, Newcastle University, Newcastle Upon Tyne, NE1 7RU, UK*

Whilst ultrafiltration has given important insights into the occurrence of colloidal metal oxides in aqueous systems, it is a time-consuming procedure and is unsuited to continuous monitoring of metal species *in situ.* A voltammetric experiment distinguishes solid-phase particles from soluble Fe species based on the greater diffusional mass transport rate of the latter. The electrochemical approach has advantages because it is rapid and there is no need to choose a filter with an arbitrary molecular mass cut-off. There have been many voltammetric studies of iron in natural waters employing stripping techniques, especially in oceanography.[14–17] However these mainly deal with trace analysis of Fe which presents different analytical challenges compared to the high concentrations typically observed in mine-affected waters. Another example is in the study of wetlands where Fe, Mn, O and S-containing species are of particular interest.[18] Some voltammetric studies of dissolved iron relevant to acid mine-water disharge have been reported, however their focus has mainly been on electrochemical remediation,[19] fundamental studies of bacterial iron respiration related to mine-water remediation,[20,21] or the development of portable equipment.[22] In this report, we show how voltammetric techniques can be employed to measure, not only total iron ($[Fe]_{total}$), but also dissolved ($[Fe]_{aq}$) and solid-phase iron ($[Fe]_{sol}$). We further show that voltammetric techniques are sensitive to aspects of iron speciation in mine-water, including the presence of hydrolysed *versus* unhydrolysed Fe ($[Fe]_{hyd}$, $[Fe]_{unh}$), and that they can be used to monitor the ratio of Fe(II) and Fe(III) redox states. Finally, through a combination of filtration and voltammetric measurements, we have been able to determine iron-containing nanoparticles in mine-waters, a topic of increasing importance.[23–25] The detailed interpretation of the biogeochemical significance of these analytical data for iron will be reported elsewhere.

2. Experimental

2.1. Reagents/chemicals

All the reagents used were of analytical reagent grade (AnalaR) and were purchased from Sigma-Aldrich Chemicals (Gillingham, UK). All electroanalytical calibration measurements were made with either 0.1 M KCl or 0.1 M Na_2SO_4 solutions in water as background electrolytes. Water used for preparation of electrolyte solutions in calibration experiments and cleaning of the electrodes was purified using a milli-(Q) Plus filter-NANOpure RO, Model D11931 (Barnstead International, Dubuque, Iowa, USA) and had a nominal resistivity of 18.2 MΩ cm.

2.2. Field analyses

pH, oxidation-reduction potential (E_h), temperature and electrical conductivity measurements were performed on-site with a Camlab 6T Ultrameter (Myron L. Company, Karlsbad, USA). On-site determination of alkalinity (expressed as mg L^{-1} of $CaCO_3$) was carried out by titration with 1.6 N sulfuric acid to an end-point at pH 4.5 using a Hach ALDT test kit (Hach Company, Loveland, USA). Bromocresol green-methyl red indicator powder was used to identify this end-point.

2.3. Collection, storage and pre-treatment of samples

Pre-washed polyethylene sample bottles (100 mL) were cleaned in 10% v/v conc. HNO_3 overnight and then rinsed thoroughly with water (×3). The bottles were then allowed to dry in air. The sampling protocols followed those used previously at the CoSTaR (Coal Mine Sites for Targeted Remediation Research) facility to ensure comparability of the data.[26] 100 mL mine-water samples were collected at each location and refrigerated at 4 °C before analysis, voltammetric measurements were carried out < 48 h after sampling. Four types of samples were collected: unacidified/acidified and unfiltered/filtered.

Acidified samples. Some samples were acidified: 1 mL concentrated HCl was added to the sample bottle before collection of a 100 mL mine-water sample. Fe-containing oxyhydroxides dissolve under these conditions and all the Fe in the sample is in solution, this sampling protocol was therefore suited to the determination of total iron, $[Fe]_{total}$. This method also limits the oxidation of Fe^{2+} and hydrolysis of Fe^{3+} during transport and storage.

Filtered samples. Some samples were filtered with 0.45 μm cellulose nitrate membranes (Whatman International Ltd, Maidstone, England) to remove > 450 nm diameter solid-phase material.

Samples which are acidified allow determination of total Fe = solid + colloidal + dissolved. Samples which are filtered contain truly dissolved and colloidal Fe: voltammetry is sensitive to the truly dissolved fraction, but if the filtered sample is acidified then all the Fe is dissolved and is detected voltammetrically.

2.4. Voltammetric analysis

All the voltammetric experiments were performed in a standard glass three-electrode cell containing 10 mL of sample solution. The cell consisted of a gold disc working electrode (2 mm diameter), platinum counter electrode and saturated calomel reference electrode (SCE; Sycopel Scientific Ltd., Washington, UK). The metal electrodes were cleaned by polishing with a dispersion of 0.05 μm alumina (Buehler, Il, USA) in water, rinsed with water, dipped in absolute alcohol (99%) and then placed in an ultrasonic bath for 2 min (Transonic T310, CAMLAB, Cambridge, UK) to remove any embedded alumina particles present. The working electrode was given a final rinse with water and blown dry with a hot-air gun. The electrochemical cell was purged with nitrogen gas to remove any oxygen that may interfere with the analysis. The working electrodes were dipped into the samples for at least 2 min prior to analysis. At least triplicate scans were performed on each sample to verify the reproducibility of the measurements and estimate uncertainties.

Cyclic voltammetry (CV) was used to investigate the Fe speciation and to understand the voltammetric responses. Differential pulse voltammetry (DPV) was used as the main analytical tool because of its superior analytical sensitivity. Two potentiostats were used: model CHI760B (CH Instruments, Austin, TX, USA) and an EG&G Princeton Applied Research Potentiostat/Galvanostat model 263A running M270 Echem Software v4.11 under MS-DOS. Our monitoring of [Fe] in

mine-waters by differential pulse voltammetry was based on the following protocol: potential scan +0.8 V → −1.2 V; 75 mV pulse height, 50 ms pulse width and a scan increment of 2 mV.

Steady-state voltammetry was carried out at a 50 μm radius Pt disc microelectrode (UME) and the same counter and reference electrodes as for CV and DPV measurements above. The UME was prepared by sealing 100 μm diameter Pt wire (Goodfellow, Cambridge, UK) in a 2 mm glass capillary under vacuum. Contact was made using Hg and a copper wire. The electrochemical cell was purged with nitrogen gas to remove any oxygen as for CV and DPV. The scan rate was typically 10 mV s^{-1} or less to ensure near steady-state behaviour of the voltammograms. The ratio of Fe(II) to Fe(III) was obtained from the anodic and cathodic diffusion limited currents under the normal assumption that the diffusion coefficients of Fe(II) and Fe(III) are equal.

2.5. Inductively-coupled plasma-optical emission spectroscopy (ICP-OES)

ICP-OES data for the total Fe content of the mine-waters were obtained using a Varian Vista-MPX ICP-OES to analyse acidified samples. The procedures have been described previously.[26,27] Because these samples were not generally filtered prior to acidification, most of the ICP-OES results reported here are total concentrations ($[Fe]_{total}$). The relative accuracy of these measurements, expressed as a percentage of the measured value is about 5%. Accuracy and precision in the ICP-OES data were ensured by measuring an AQC (Aqueous Quality Control) standard at regular intervals (typically every 5 samples) during analyses. This ensured that the instrument was stable and the measured values did not drift. The AQC standard was made-up by diluting commercially available stock solutions (1000 mg dm^{-3}). The stock solution of AQC was purchased from VWR International Ltd., Poole, BH15 1TD, England. The analytical results are recorded only if the AQC standards check is with ±5% of the nominal values. Certified Reference Material (CRM) was not used in this analytical procedure due to problems with obtaining a standard of the same Fe level as the CoSTaR mine-waters. To the best of our knowledge, there are no suitable CRM standards for mine-water.

2.6. Atomic force microscopy

Atomic force microscopy (AFM) imaging was performed using a Nanoscope IIIa/Multimode atomic force microscope in tapping mode™ (Digital Instruments Santa Barbara, CA, USA). Samples for AFM were prepared by allowing a small volume (typically 0.1 mL) of mine-water to dry overnight on cleaved mica samples.

2.7. Electron microscopy and elemental analysis

SEM: The scanning electron microscope (SEM) was a LEO 1530 Gemini SEM column, fitted with a field emission gun (FEG) source. Small portions (a few mg) of solid samples (from dried mine water samples) were placed on conductive carbon pads and then mounted onto a standard aluminium SEM stub and sprayed with compressed air (Clean Air Duster; Kenair, Swindon, UK). The sample was coated with 3 nm of Pt/Pd metallic film (80% : 20%) using a high resolution sputter coater (Agar Scientific Ltd.) and loaded in the specimen chamber. Images were acquired with the FEG-SEM operating at an accelerating voltage of 3 kV and using a solid state detector at the pole piece of the objective lens to generate images with good surface detail. High purity nitrogen was used to vent the chamber when changing specimens in order to prevent water vapour from contaminating the column.

TEM: The drop-casting technique was used for sample preparation. A few milligrams of samples were dissolved in an organic solvent (ethanol < 1 mL) and mixed by sonication for 2 mins. A drop of this mixture was deposited on the TEM grid (3 mm diameter). The TEM grid was a 400 mesh Cu support grid with a 30 nm thick amorphous 'holey' carbon film laid across it (Agar Scientific Ltd). The thin specimens were then examined using a Philips CM200 FEG-TEM operated at 197 keV equipped with scanning (S)TEM capability and fitted with an Oxford Instruments ultra thin window energy dispersive X-ray spectrometer (EDX) and a Gatan (GIF 200) imaging filter (used for digital imaging but with electron energy loss spectroscopy capability). Elemental mapping was done by scanning transmission electron microscopy (STEM) combined with EDX.

2.8. Mine-water sampling sites

A brief description of the sites from which we sampled mine-affected waters is given here. The CoSTaR facility comprises several polluted former mines at various locations across NE England. It includes six, full-scale, passive mine-water treatment systems, based upon experimental wetland-creation schemes.[28–32] The sites comprise six bioreactors, including a permeable reactive barrier (PRB), a compost wetland, a reducing and alkalinity producing system (RAPS) and four varieties of aerobic wetlands (receiving a range of acidic and alkaline mine waters with peroxide pre-dosing in one case).

Water samples are regularly obtained at a number of sampling points in all these locations. These samples are analysed for acidity, E_h, temperature, conductivity and, total Fe content ($[Fe]_{total}$). $[Fe]_{total}$ is determined by atomic spectroscopy, specifically ICP-OES. The spectroscopic data is obtained on samples that are acidified to dissolve solid-phase iron and do not provide any direct information on the quantity of colloidal iron or the speciation and redox states of iron in the various parts of the CoSTaR sites.

3. Results and discussion

The voltammograms of Fe(II) and Fe(III) in aqueous calibration solutions, as well as the mine-water samples, show at least three peaks. It is well known that the speciation of Fe aquo ions is complex: extensive hydrolysis of Fe(III), leading eventually to precipitation of oxyhydroxides, occurs unless the solution is strongly acidic. Most physicochemical studies of $Fe_{(aq)}$ voltammetry are carried out in strong acid solutions to suppress the hydrolysis.[33] However, the pHs observed in our samples vary substantially from 2.85 to 7.90. We therefore discuss briefly the effect of the hydrolytic reactions on the voltammetry that we observe in the mine-water samples, before describing the analytical results. Difference measurements on acidified and unacidified samples enables a simple determination of the

amount of solid phase Fe present in the samples and, by filtering samples before acidification, we can determine Fe present in nanoparticulate form. Finally, we present a simple microelectrode technique to determine the ratio of Fe(II)/Fe(III) oxidation states in the soluble Fe fraction.

3.1. Speciation of Fe(III) and Fe(II)–voltammetric studies

The standard potential for the electrode reaction,

$$Fe(H_2O)_6^{3+} + e^- \rightleftharpoons Fe(H_2O)_6^{2+}$$

is +0.77 V *vs.* SHE, or about +0.53 V *vs.* SCE. However, $[Fe(H_2O)_6]^{3+}$ is acidic and the pK_as for the first two deprotonation steps are 2.19 and 5.67.[34] There may therefore be significant amounts of $[Fe(H_2O)_5OH]^{2+}$ and $[Fe(H_2O)_4OH_2]^{+}$ in the mine-water samples. Since the pK_a for $Fe(H_2O)_6^{2+}$ is 9.5,[35] Fe(II) species in the mine-waters will mostly be unhydrolysed. In our voltammetric experiments, the reduction of $[Fe(H_2O)_6]^{3+}$ and its conjugate bases will appear as a single wave (or peak) because the proton transfers to oxygen are fast on the voltammetric timescale. However, because of the difference in pK_a between the Fe(III) and Fe(II) oxidation states, the wave will shift in a negative direction when the pH increases, as we observe. We therefore assign the most positive peak potential in the voltammograms to the reduction of the Fe(III) hexaaquo ion, its conjugate base and any other species in rapid equilibrium with it. In Fig. 1, this peak is labelled (i) and the concentration of the species contributing to it is denoted $[Fe]_{unh}$.

The most negative peak is labelled (iii) in Fig. 1: it is clearly due to electrodeposition of Fe by reduction of Fe(II). This is evident from the presence of a nucleation loop in the CV (Fig. 1iv) and the presence of a characteristic stripping peak (Fig. 1v). If the potential scan is reversed before peak (iii) (Fig. 1, dashed line), no stripping peak is observed, which confirms that peak (Fig. 1iii) is due to the electrodeposition of Fe.

This leaves the question of the assignment of the peaks (Fig. 1ii) at intermediate potentials. First, we note that the effect of dissolved oxygen in voltammetric studies of Fe has been studied,[22] but in our experiments we have purged the solutions with nitrogen and therefore these peaks are not related to oxygen reduction. In the concentration range 1–10 mM, the formation of significant quantities of dinuclear and multinuclear Fe species is known and is responsible for the reddish colour of aqueous Fe(III).[36–40] The hydrolysis of Fe(III) has been extensively investigated, but the precise description of the species present is still the subject of discussion:[37–46] the two major proposals for the structure of the dimeric iron species are $[Fe_2(\mu\text{–}OH)_2(H_2O)_8]^{4+}$ and $[Fe_2(\mu\text{–}O)(H_2O)_{10}]^{4+}$. A combined quantum chemical and electronic spectroscopy study has provided evidence in support of the more commonly quoted bis(μ-hydroxo) form.[42] X-ray absorption fine structure spectroscopy is consistent with this picture at low pH, the spectra were used to derive Fe–Fe coordination numbers and were assigned to edge sharing octahedral Fe units.[43] The presence of higher oligomers was detected at pH > 3, but, importantly for environmental samples, the presence of silica was found to inhibit oligomerisation of Fe species. It is known that the Fe aqua dimer is kinetically stable in mildly acidic solutions (pH ≃ 2) and in the presence of excess $[Fe(H_2O)_6]^{3+}$ and $[Fe(H_2O)_5OH]^{2+}$.[40–45] The break-up of the aqua dimer into monomeric Fe species has been shown to follow a rate law, rate = (0.4 s^{-1} + 3.1 M^{-1} $s^{-1}[H^+]$)[dimer].[47,48] This rate is sufficiently slow for the reduction of the aqua dimer to appear as a separate wave in our voltammetric experiments. We therefore assign the voltammetric waves (ii) at intermediate potentials to the reduction of the aqua dimer and possibly also higher nuclearity species and/or complexes with sulfate. The concentration of the species contributing to the peaks (ii) is denoted $[Fe]_{hyd}$ below.

In summary, we use peak (i) in the voltammorgams to determine unhydrolysed $[Fe(H_2O)_6]^{3+/2+}$ and its conjugate bases and we use peaks (ii) to determine hydrolysed iron species which are expected to be dimers and other low molecular weight oligomers and their conjugate bases. Neither CV nor DPV measurements provide a straightforward means to determine the redox states of either of these species, this was accomplished using steady-state microdisc voltammetry (below). Finally, although hydrolysed species such as the Fe aqua dimer are thought to be thermodynamically unstable with respect to FeOOH(s) and monomeric Fe species,[49] the slow kinetics of the system mean the use of thermodynamic arguments based on, *e.g.*, E_h–pH diagrams, to predict the actual composition of mine-water samples must be applied with caution.

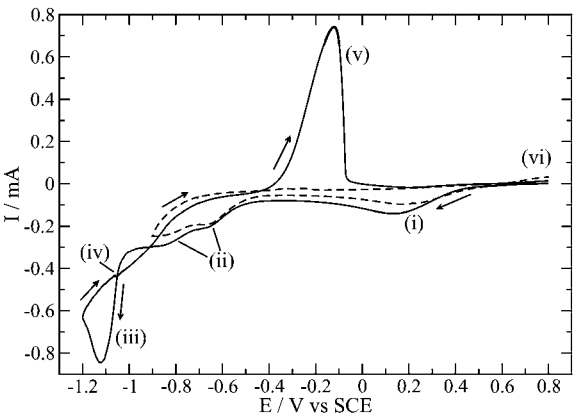

Fig. 1 Two cyclic voltammograms of 5 mM $FeCl_3$ in 0.1 M KCl (aq). The scan rate was 0.1 V s^{-1}, the working electrode was a 2 mm diameter Au disc and the reference electrode was an SCE. Various peaks of interest are labelled (i)–(v) and their assignments are discussed in the text.

3.2. Voltammetric analysis of dissolved Fe in mine-waters

Fig. 2 shows representative differential pulse voltammograms (DPVs) over the potential range corresponding to the peaks due to (i) unhydrolysed ($[Fe]_{unh}$; $E^\circ \simeq 0.45$ V) and (ii) hydrolysed Fe species ($[Fe]_{hyd}$; $E^\circ \simeq -0.2 \rightarrow -0.3$ V) in mine-water samples from a selection of sampling points across the mine sites examined in this study. The DPVs are substantially simpler in appearance than the cyclic voltammograms, even of laboratory calibration solutions (Fig. 1). Nevertheless, it is clear from the peak currents, potentials and even wave-shapes that the concentration and speciation of dissolved Fe varies substantially between sampling locations and CoSTaR sites. The pH at the various sampling points and sites is also different and this causes a shift in the voltammetric peak potentials because of the protonation equilibria of Fe(II/III) aquo ions and the extent of

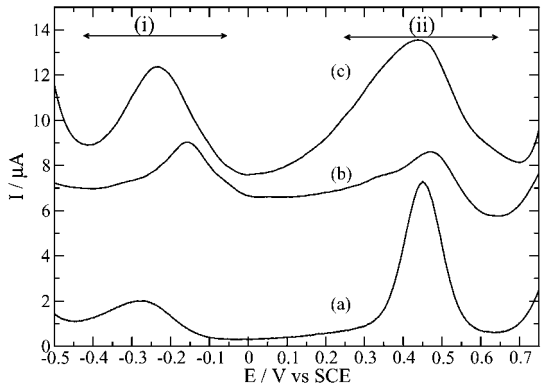

Fig. 2 Differential pulse voltammograms of unfiltered, unacidified mine water samples taken from: (a) Bowden Close site, Co Durham, pH 4.52; (b) Acomb site, Hexham, pH 6.43; (c) Shilbottle site, Northumberland, pH 3.10. DPV parameters: pulse width = 50 ms; pulse height = 75 mV and step height = 2 mV. The working electrode was a 2 mm diameter Au disc and an SCE reference electrode was used. (i) and (ii) indicate the approximate potential ranges where the voltammetric peaks for unhydrolysed and hydrolysed iron aquo species are observed.

hydrolysis of Fe(III). $[Fe]_{unh}$ as determined by a voltammetric method includes not only $[Fe(H_2O)_6]^{3+}$, but also species obtained by rapid proton transfer equilibria such as $[Fe(H_2O)_5OH]^{2+}$. As discussed in the previous section, the fraction of dissolved Fe we denote $[Fe]_{hyd}$ comprises species such as the Fe aquo dimer and perhaps higher oligomers along the pathway towards FeOOH(s).

Water samples taken at inlet and outlet locations at different mine sites varied substantially in pH and E_h (Table 1). The pH of inlet samples ranged from 2.85 to 6.81 across all sites, while samples from outlets ranged from 3.33 to 7.90. Although there is an overlap in the pH ranges of sites, outlet samples generally had higher pH than their corresponding influent samples. The E_h values of outlet samples were typically lower than the E_h of inlet samples: the observed trend is probably due to the aerobic environment of the influent and the anaerobic nature of the wetlands. Two exceptions to the general trend were found at the Quaking Houses and Whittle sites. Solid-phases such as FeOOH are expected to be thermodynamically stable at nearly all the measured E_h and pH values, nevertheless substantial dissolved Fe was found (Fig. 2) and clearly the samples are out of equilibrium in this respect.

[Fe] in all the samples studied in this report is much larger than voltammetric detection limits and several orders of magnitude greater than [Fe] measured in marine environments see, *e.g.*, ref. 50. However, the analytical challenge is to develop a simple method to quantify dissolved and colloidal Fe species that is capable of being applied on-site. In addition, owing to the large datasets (multiple sampling locations and sites, long-term pollution monitoring) the method should be simple to calibrate and involve the minimum of data processing.

Table 1 Representative pH and E_h measurements of the inlet (polluted) and outlet (treated) waters at several mine sites. In general, there is an increase in pH and, with the exceptions of the Whittle and Quaking Houses sites, a decrease in E_h upon treatment of the mine-waters

Site	Inlet pH	Outlet pH	Inlet E_h/mV	Outlet E_h/mV
Bowden Close	4.33	6.90	220	170
Shilbottle	2.85	3.33	550	470
Quaking Houses	6.26	6.55	30	60
Whittle	6.81	7.90	−120	−50
Acomb	5.51	7.07	260	210

At the values of $[Fe]_{total}$ found in mine-water, Fe(III) aquo ions are almost always deprotonated, but because the protonation reactions are rapid, these species all contribute to the peak at *ca.* 0.45 V *vs.* SCE. For simplicity we denote this fraction as $[Fe]_{unh}$ and refer to it as unhydrolysed. A significant other fraction is likely to be present as dimers or higher oligomers formed by hydrolysis of the deprotonated Fe(III) aquo ions (peak at *ca.* −0.3 V *vs.* SCE) and we denote this as $[Fe]_{hyd}$ and refer to it as hydrolysed Fe. The simplest calibration of the voltammetric responses that yields reliable $[Fe]_{total}$ is based on measurement of the peak currents due to $[Fe]_{unh}$ and $[Fe]_{hyd.}$ Because $Fe(II)_{aq}$ and $Fe(III)_{aq}$ hydrolyse to different extents, calibration solutions prepared with a constant $[Fe]_{total}$, but varying Fe(II)/Fe(III) ratios produce a range of values of $[Fe]_{unh}$ and $[Fe]_{hyd.}$ Over the range of conditions of pH and $[Fe]_{total}$ that we encountered, a simple linear calibration sufficed:

$$I_{peak}(i)/\mu A = 8.8(1)\{[Fe]_{unh}/\text{mmol dm}^{-3}\} + 1.8(1) \quad (5)$$

$$I_{peak}(ii)/\mu A = 9.9(9)\{[Fe]_{hyd}/\text{mmol dm}^{-3}\} + 0.49(1) \quad (6)$$

The total dissolved Fe was obtained by adding the concentrations of hydrolysed and unhydrolysed Fe: $[Fe] = [Fe]_{unh} + [Fe]_{hyd}$. We have validated our method by comparison of [Fe] from DPV to ICP-OES data, with which we obtained satisfactory agreement, as discussed below.

Fig. 3(a) and 3(b) show comparisons of [Fe] for both unfiltered and filtered samples as measured by DPV and by the ICP-OES method used previously[26] for the portion of our full dataset where we have both ICP-OES and DPV measurements. Out of a full dataset of about 1000 samples, we have 298 measurements in Fig. 3(a) and 95 measurements in Fig. 3(b). The most concentrated samples correspond to about 0.1 M (by ICP) and the most dilute to 2×10^{-5} M (by ICP). The correlation between the two datasets is clear and the values of r^2 are 0.94 and 0.92 for the unfiltered and filtered samples based on the log–log plots. The voltammetric data for samples which are unfiltered, but acidified clearly determine total Fe in reasonable agreement with ICP-OES. The samples which are filtered first, then acidified determine total Fe of particle size <450 nm and dissolved Fe. There are however, several outlying data points where the voltammetric analysis differs a great deal from the spectroscopic analysis. If we define as outliers those data points where the absolute percentage deviation of the voltammetric analysis from the atomic spectroscopy analysis is > 50% and remove the outliers from the data of Fig. 3, then the mean percentage deviations are −2.6% and 0.6% for unfiltered and filtered samples respectively. In fact, most of the outliers, especially those at high $[Fe]_{total}$ derive from one particular site, at Shilbottle, Northumberland where the highest Fe concentrations are observed. The agreement between voltammetry and atomic spectroscopy is best in the intermediate range of 10^1–10^3 mg Fe L^{-1} with the voltammetric measurements being systematically slightly smaller

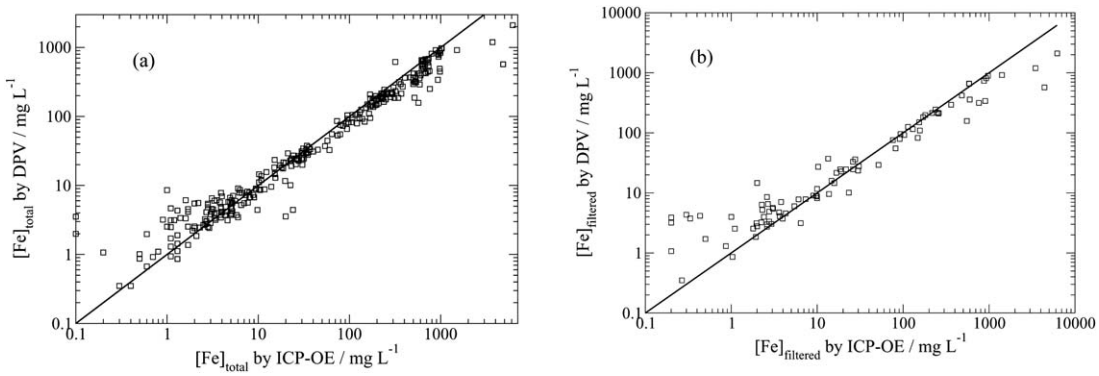

Fig. 3 Comparison of [Fe] determined by DPV and ICP-OES for (a) unfiltered (total Fe) and (b) filtered samples with acidification (dissolved + colloidal Fe). The datasets shown comprise samples taken from all the CoSTaR sites over a full season of monitoring (March 2006 to April 2007). The solid lines are a guide to the eye; measurements lying on this line correspond to exact agreement between DPV and ICP-OES analyses.

in this range (about −3% deviation). In the filtered samples, at the lowest [Fe] < 10 mg Fe L^{-1} there is some evidence that the voltammetric measurements are systematically higher.

Estimates of the limit of detection for our voltammetric method can be made by a linear regression analysis of the data in Fig. 3. After excluding data points from the Shilbottle site at high [Fe] which gives the worst correlation between the methods (for reasons indicated below), we find the best fit slope (mean ± standard error) for the [Fe] total data is 0.84 ± 0.013 and for the filtered data we obtain 0.89 ± 0.027 (Fig. 4). As expected on general grounds, the electrochemical method gives a best fit slope closer to 1 for the filtered data where interferences from the sample are minimized. The corresponding estimates of the *y*-intercept of the regression line are 1.1 ± 0.8 and 2.2 ± 1.5 mg L^{-1}. These values allow us to estimate $[Fe]_{total}$ and $[Fe]_{filtered}$ by DPV when [Fe] =0 by the established ICP method. Using these values, we estimate the detection limit (LOD) to be about 2.8 mg L^{-1} (total) and 4.9 mg L^{-1} (filtered) based on the common prescription of taking 3× standard deviation of the blank. Fig. 4 shows an alternative presentation of the data in which the percentage deviation of the measured values from the regression line is plotted against the [Fe] by ICP; the percentage deviations increase substantially at $[Fe]_{filtered}$ < 5 mg L^{-1}. This is substantially in agreement with our estimate of the LOD based on the regression analysis of the filtered dataset, but suggests that the value of 2.8 mg $L^{-1}$for the total Fe dataset is probably too optimistic.

Finally, we show two examples of datasets that illustrate: (Fig. 5) a typical site where the total [Fe] is within the range 10^1–10^3 mg Fe $L^{-1}$and (Fig. 6) another site where very high total [Fe] values are occasionally observed and there are location-specific reasons for the worse analytical performance.

Fig. 5 shows a typical set of data for one mine site and compares our DPV measurements of total dissolved Fe compare with the ICP-OES method. The two methods agree within the 10% uncertainties associated with the ICP data. The data presented in Fig. 5 is representative of the general trend observed when we compare DPV and ICP-OES for sites with [Fe] in the range 10^1–10^3 mg Fe L^{-1}. An example of a site where there is significant discrepancy between the two analyses is Shilbottle, which shows extremely high [Fe] because the pollution at this site is mine soil-heap leachate. The correlation between the DPV and ICP-OES data remains clear, although the quantitative agreement is not as good (Fig. 6). The agreement is poorest for the underground mine-water samples, which contain more organic and particulate matter that may decrease the voltammetric signals by complexation of Fe or by fouling the electrode. It is an advantage of ICP in a purely analytical context that organic matter is destroyed in the plasma and does not affect [Fe], however Fe complexed to organic ligands may have a significant role in the geochemistry of acid mine drainage.

3.3. Voltammetric analysis of solid phase Fe species in mine-waters

In the previous section we reported on the analytical performance of the voltammetric technique with respect to the established ICP method. In this section we show that, despite the limitations discussed above, the electrochemical method is capable of observing the variations in [Fe] of interest in a study of mine-waters. Further, we also show that the technique can be used to estimate the nanoparticulate fraction of Fe in these samples and, by presenting some illustrative datasets, has the capability to track changes in these values across different sites and over time.

Fig. 7 and 8 show that acidification of samples changes the voltammetric peak currents for hydrolysed and unhydrolysed Fe; these values increase and approach the values determined by ICP-OES and the difference is due to dissolution of solid-phase Fe in acidified samples. Filtered samples also gave increased values on acidification and based on these measurements, up to 30% of the solid phase Fe consists of particles less than 0.45 μm (the filter cut-off) depending on the sampling locations and sites. The voltammetric method does not have a sharp particle size cut-off, instead it distinguishes solid phase and freely-diffusing Fe based on their diffusion coefficient (*D*), because the peak currents in CV and DPV are proportional to $D^{1/2}$. In practice, however, the voltammetric method acts similar to filtration with an extremely fine filter, because the voltammetric signals for even 10 nm Fe-containing particles are negligible compared to the peak currents for the equivalent concentrations of truly dissolved Fe.

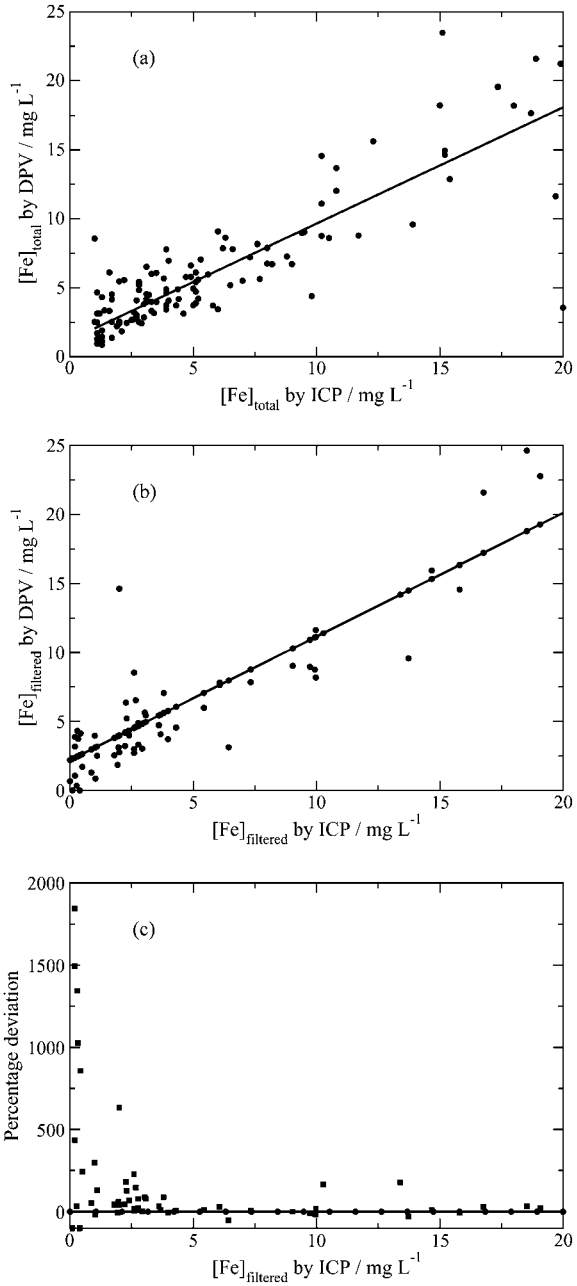

Fig. 4 Linear regression of the datasets of Fig. (3). (a) Total Fe, (b) Filtered samples and (c) percentage deviation of the $[Fe]_{filtered}$ by DPV against $[Fe]_{filtered}$ by ICP. The data in part (c) shows that for $[Fe]_{filtered}$ by ICP < 5 mg L^{-1} the percentage deviations become large.

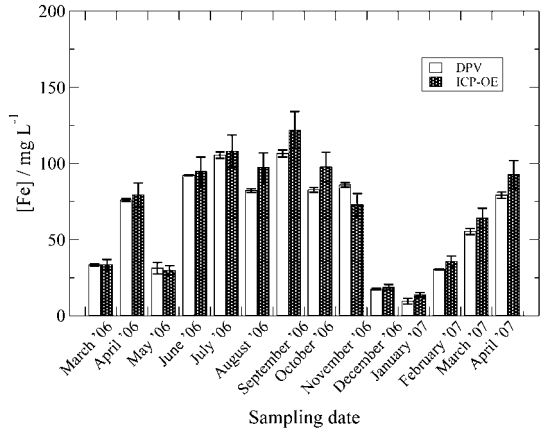

Fig. 5 Comparison of total [Fe] measured by DPV and ICP for unfiltered aquifer/surface mine water samples taken from the Bowden Close site. The electrochemical total Fe concentrations were obtained by adding the concentrations of hydrolysed and non-hydrolysed Fe determined by differential pulse voltammetry. The ICP-OES values are known to have an uncertainty of 5–10%. The error bars on the DPV data are 95% confidence intervals: these uncertainties are discussed in the text. In both cases (voltammetry and ICP methods), the samples were acidified with 1% v/v HCl to remove solid Fe oxyhydroxides.

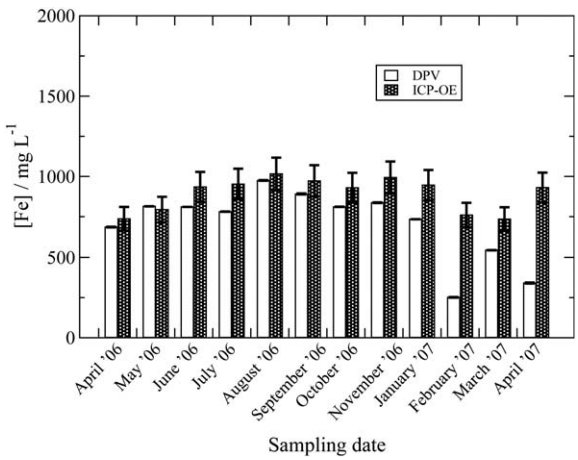

Fig. 6 Comparison of total Fe/mg L^{-1} measured by DPV and ICP-OES by acidification of unfiltered underground mine-water samples at the Shilbottle site.

By comparing the voltammetric analysis in filtered, but unacidified samples with that in filtered, acidified samples we can estimate the concentration of Fe present in particles below our filter cut-off of 0.45 μm. This fraction is referred to as nanoparticulate Fe and we find that it comprises a substantial portion of the Fe present, on average 34% of the Fe that passes the filter is in fact nanoparticulate rather than truly dissolved Fe (Fig. 9).

Comparison of Fig. 8(a) and 8(b) shows that CVs of acidified mine-water samples have the normal voltammetric wave shape for pure laboratory reagents in the region denoted $[Fe]_{unh}$, whilst CVs for unacidified mine-water samples are rather broad. This is mainly a result of the additional complexitiy of Fe speciation in mine-water with various organic ligands and other dispersed solid phases present. Although the acidification also decreases the solution resistance, the conductivity of the unacidified samples is already > 1 mS cm^{-1} in the majority of cases and uncompensated resistance effects are not expected to be large for the observed currents which are of the order of 1μA. In a similar manner, the DPVs of acidified and unacidified samples as shown in Fig. 8(c) and 8(d) also revealed 'sharp' peaks for acidified samples whilst peaks for unacidified samples are somewhat broad and much smaller. In fact, Fig. 8(d) is an example where there is very little dissolved Fe present before acidification. The overall characteristics of the peaks are also defined by the original pH of the mine-water samples concerned. For example, an

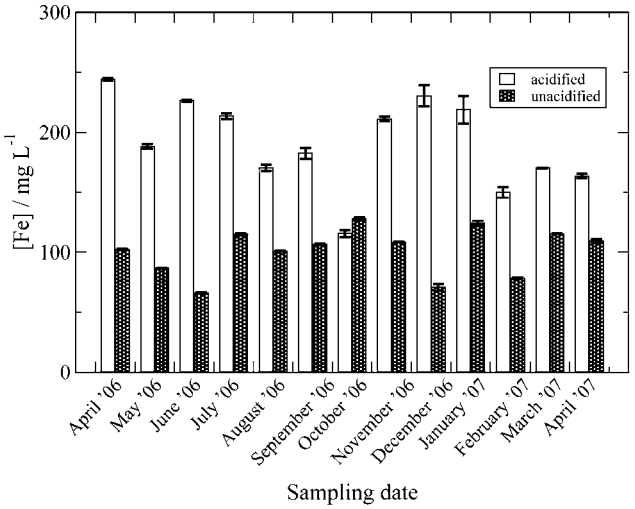

Fig. 7 A typical dataset (from Bowden close) showing a comparison of Fe/mg L^{-1} concentrations measured from the acidified and unacidified samples. The differences indicate the proportion of solid phase Fe.

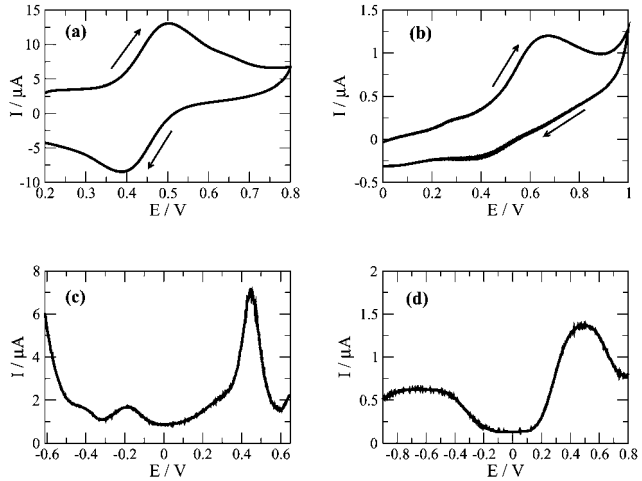

Fig. 8 Representative cyclic and differential pulse voltammograms of unfiltered mine-water samples with and without acidification. All these samples were taken from the RAPS2 inlet of the Bowden Close site: (a) CV of acidified sample; (b) CV of unacidified sample; (c) DPV of acidified sample and (d) DPV of unacidified sample. CV parameters: scan rate = 0.1 V s^{-1}; DPV parameters: pulse width = 50 ms; pulse height = 75 mV and step height = 2 mV. The working electrode was a 2 mm diameter Au disc and an SCE reference electrode was used.

unacidified mine-water sample with a pH of 3–5 normally showed sharp and symmetric peaks for both CV and DPV whilst mine-water samples with pH of 5 upward normally showed broad and asymmetric peaks for both CV and DPV. These effects cannot be accounted for by a simple linear calibration such as eqn (5) and (6). This is the major source of the outlying points in Fig. 3(a) and 3(b). It also suggests that our method for determination of nanoparticulate Fe may overestimate that component in waters of relatively high pH > 5 because the effect of acidification is not only to dissolve nanoparticulate Fe, but also to sharpen the voltammetric peaks, an effect not accounted for in our simple calibration. At present, we cannot quantify

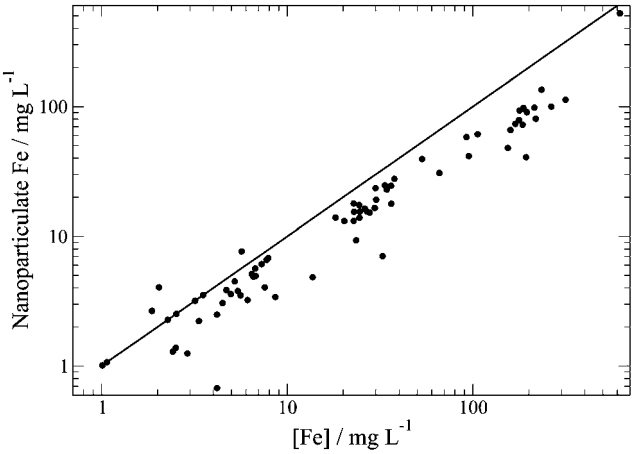

Fig. 9 Nanoparticulate Fe against truly dissolved Fe across the 6 mine sites in this study. Truly dissolved Fe was determined by analysis of filtered samples (0.45 µm cut-off) and nanoparticulate Fe was estimated by the increase in voltammetric signals upon acidification of the filtered samples. The line indicates measurements for which the two concentrations are equal.

these effects because of the complex changes in the voltammetric wave-shapes.

In order to confirm the presence of nanoparticles containing Fe, direct observations of the nanoparticles in the mine-waters were made by atomic force microscopy (AFM). Fig. 10 shows a typical tapping mode AFM image of the particles remaining when a few µL of a filtered sample was allowed to dry on a cleaved mica surface. Unfiltered samples contained too much colloidal material with too high a mean particle size (order of µm) for AFM imaging. However, the image does show that there is a significant amount of nanoparticulate matter in the filtered samples (diameters of order tens of nm). Electron microscopy (Fig. 11) also revealed the presence of such nanoparticles and elemental mapping by EDX and STEM confirmed the presence of Fe in these particles.

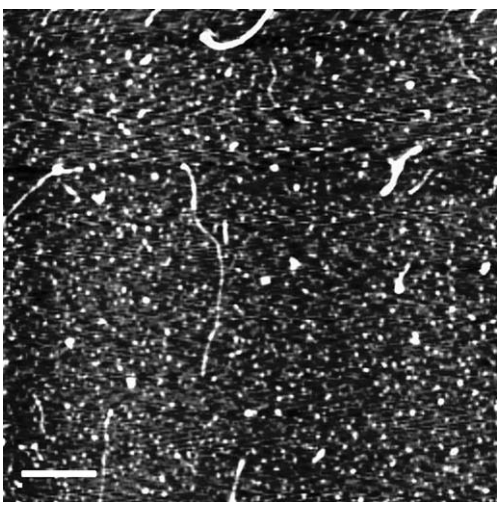

Fig. 10 AFM image of particles deposited on mica. The scale bar represents 500 nm and the grayscale corresponds to a height of 3 nm (black-white). The majority of the particles observed (white spots) have diameters of the order of a few tens of nm.

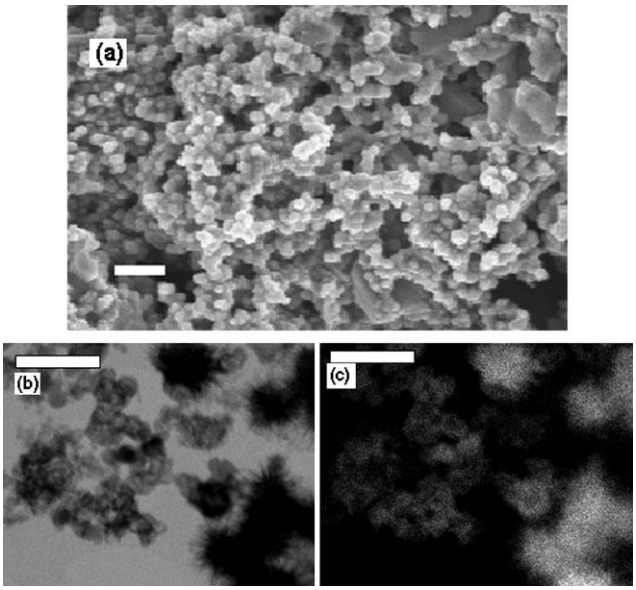

Fig. 11 (a) Typical scanning electron micrograph of particles present after drying mine water samples from the Shilbottle site (the scale bar represents 300 nm); (b) Bright field HR-TEM image of particles from the Shilbottle site and (c) corresponding Fe elemental map of the sample in (b). The scale bar in (b) and (c) represents 500 nm.

3.4. Voltammetric determination of the oxidation states of dissolved Fe species in mine-waters

DPV is not suited to the determination of oxidation states because the same symmetric peak shape is observed irrespective of scan direction and therefore the voltammograms are the same irrespective of whether the bulk solution contains Fe(II) or Fe(III). In principle, a CV experiment can be used to determine the ratio of oxidised/reduced species because the transient current observed at the start of the sweep depends on the composition of the bulk solution. However, analysis of this current requires a calculation of the time-dependent wave-shape; steady-state voltammetry also provides this information, but in a simpler manner. The diffusion-limited anodic (cathodic) currents in a steady-state voltammogram are proportional to the bulk concentrations of reduced (oxidised) forms of the redox couple. In the mine-waters there are at least two dissolved Fe species and therefore multiple diffusion-limited currents are expected. Fig. 12 shows a near steady-state microelectrode voltammogram, typical of those we have observed in mine-waters.

On the negative-going scan, a wave is observed at about +0.1 V and a second, larger wave at about −0.5 V. Based on similar arguments used to interpret the DPV, we assign the two waves to the reduction of unhydrolysed Fe at +0.1 V and the reduction of the hydrolysed Fe at −0.5 V. We have therefore taken the limiting anodic current at potentials >0.1 V to be proportional to $[Fe(II)]_{unh}$ and the limiting cathodic current as proportional to $[Fe(III)]_{unh.}$ However this interpretation does require an assumption about the wave at −0.5 V, namely that this is entirely due to reduction of $[Fe(III)]_{hyd}$, otherwise it is not possible to assign the current between +0.1 V and −0.5 V entirely to reduction of $[Fe(III)]_{unh.}$ This assumption is reasonable given the

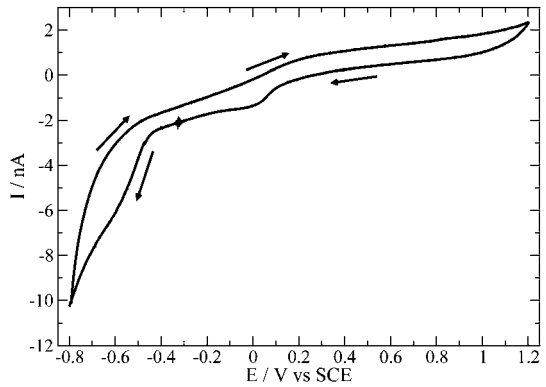

Fig. 12 Typical microelectrode voltammogram of unfiltered, unacidified mine-water. The electrode was a 50 μm radius Pt inlaid disc, the reference electrode was an SCE and the scan rate was 10 mV s^{-1}.

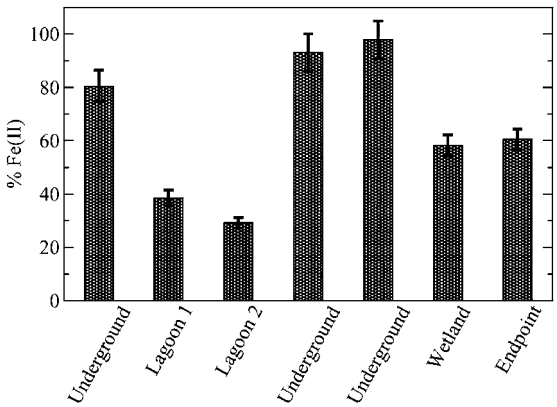

Fig. 13 Percentage of dissolved, unhydrolysed iron present as Fe(II). Samples taken from the Shilbottle site, March 2008. The sampling locations are either underground (anaerobic environment) wetlands (reducing) or more aerobic environments such as the settlement lagoons. The error bars represent the standard deviation based on triplicate measurements (about 7%).

known chemistry of Fe aquo ions: the pK_a of $Fe(H_2O)_6^{2+}$ is 9.5, which is higher than the pH of any of our samples (Table 1), so hydrolysed Fe(II) is unlikely to be present, it would have to originate in the reduction of hydrolysed Fe(III) species. There are no data on Fe(II)/Fe(III) ratios comparable to the ICP-OES determinations of [Fe] against which we can compare our UME data. However, we can study the variation of the Fe(II)/Fe(III) ratio at different sampling locations and show that the gross features of the data are in line with expectations based on geochemical knowledge of the site. Fig. (13) is a typical example: in brief, water sampled from reducing or anaerobic environments such as wetlands and underground locations tends to be rich in Fe(II). A detailed account of the geochemistry is outside the scope of this article and will be published elsewhere.

4. Conclusion

After addition of acid to samples taken from mine-water remediation sites, DPV yields results for [Fe] in substantial agreement with ICP-OES, the standard analytical method in this

application. Detailed comparison of both methods (atomic spectroscopy *vs.* electrochemical) over a period of 14 months, across 6 sites and a total of 59 sampling locations shows that the total Fe concentrations determined by ICP are systematically higher than those measured electrochemically at locations in the most polluted site (Shilbottle) at which there is a large fraction of suspended solids and organic matter. Nevertheless, we are able to determine soluble Fe by DPV in many untreated (no addition of acid) mine-waters and, by difference, the solid phase Fe. AFM of some of the solid material remaining after drying filtered samples shows that there is a significant amount of Fe-containing colloidal particles with size of order of a few tens of nanometres. This fraction of the solid-phase Fe is not conveniently removed, except by ultrafiltration methods, and therefore the voltammetric experiment offers practical advantages for its quantitation by filtering the samples with a 0.45 μm filter prior to acidification. The simple electrochemical method reported here has enabled the speciation of dissolved Fe and the quantitation of solid phase/nanoparticulate Fe in the polluted mine-water samples across the mine sites and the observation of trends in both soluble and solid phase Fe over a period of 14 months. This dataset (59 sampling locations across 6 sites) provides a valuable resource for the understanding of the factors controlling the efficiency of mine-water remediation in these sytems. In addition, steady-state voltammetry at microdisc electrodes was found to provide a simple means to discriminate the important redox states Fe(III) and Fe(II) and this technique was applicable directly in mine-waters to the soluble fraction of the Fe.

5. Acknowledgements

We thank the HERO group at Newcastle University for access to data and help in sampling. Some of the data presented here have been collected under the auspices of the CoSTaR facility, which was funded by an EU-FP6 Access to Research Infrastructure grant.

References

1 P. L. Younger, *Sci. Total Environ.*, 1997, **194–195**, 457–466.
2 P. L. Younger, S. A. Banwart and R. S. Hedin, *Mine Water: Hydrology, Pollution, Remediation*, Kluwer Academic Publishes, The Netherlands, 2002.
3 C. A. J. Appelo and D. Postma, *Geochemistry, groundwater and pollution*, 2nd edition, A.A. Balkema, Leiden, 2006 pp 450–452.
4 T. D. Mayer and W. M. Jarrell, *J. Environ. Qual.*, 1995, **24**, 1117–1124.
5 B. A. Kimball, E. Callender and E. V. Axtmann, *Appl. Geochem.*, 1995, **10**, 285–306.
6 J. M. Ross and R. M. Sherrell, *Limnol. Oceanogr.*, 1999, **44**, 1019–1034.
7 L. E. Schemel, B. A. Kimball and K. E. Bencala, *Appl. Geochem.*, 2000, **15**, 1003–1018.
8 D. M. Hill and A. C. Aplin, *Limnol. Oceanogr.*, 2001, **46**, 331–344.
9 T. Allard, N. Menguy, J. Salomon, T. Calligaro, T. Weber, G. Calas and M. F. Benedetti, *Geochim. Cosmochim. Acta*, 2004, **68**, 3079–3094.
10 E. Boyle, J. M. Edmond and E. R. Sholkovitz, *Geochim. Cosmochim. Acta*, 1977, **41**, 1313.
11 O. S. Pokrovsky and J. Schott, *Chem. Geol.*, 2002, **190**, 141–179.
12 E. R. Sholkovitz and D. Copland, *Geochim. Cosmochim. Acta*, 1981, **45**, 181–189.
13 G. Deein, W. Thimdee and K. Matsunaga, *Mar. Freshwater Res.*, 2002, **53**, 43–47.
14 A. Bobrowski, K. Nowak and J. Zareogonbski, *Anal. Bioanal. Chem.*, 2005, **382**, 1691.
15 R. Segura, M. I. Toral and V. Arancibia, *Talanta*, 2008, **75**, 973–977.
16 C. M. G. van den Berg, *Anal. Chem.*, 2006, **78**, 156–163.
17 M. Boye, A. Aldrich, C. M. G. van den Berg, J. T. M. de Jong, H. Nirmaier, M. Veldhuis, K. R. Timmermans and H. J. W. de Baar, *Deep-Sea Res., Part I*, 2006, **53**, 667–683.
18 S. Ma, G. W. Luther III, J. Keller, A. S. Madison, E. Metzger, J. P. Megonigal and D. Emerson, *Electroanalysis*, 2008, **20**, 233–239.
19 T. L. Hatfield and D. T. Pierce, *J. Appl. Electrochem.*, 1998, **28**, 397–403.
20 A. A. Bilgin, J. Silverstein and M. Hernandez, *Environ. Sci. Technol.*, 2005, **39**, 7826–7832.
21 F. Baldi, D. Marchetto, D. Battistel, S. Daniele, C. Faleri, C. De Castro and R. Lanzetta, *J. Appl. Microbiol.*, 2009, **107**, 1241–1250.
22 T. Hezard, G. Durand, M. Rakib, P. Viers, S. Roy, N. Guigues, M. Brach, J. P. Heitzmann, P. Eberle and F. Bellouard, *Electroanalysis*, 2009, **21**, 1401–1410.
23 M. Hassellov and F. von der Kammer, *Elements*, 2008, **4**, 401–406.
24 G. W. Luther and D. T. Rickard, *J. Nanopart. Res.*, 2005, **7**, 389–407.
25 N. S. Wigginton, K. L. Haus and M. F. Hochella Jr, *J. Environ. Monit.*, 2007, **9**, 1306–1316.
26 A. P. Jarvis, M. Moustafa, P. H. A. Orme and P. L. Younger, *Environ. Pollut.*, 2006, **143**, 261–268.
27 APHA, 1998. *Standard Methods for the Examination of Water and Wastewater, 20th Edition. American Public Health Association.* American Water Works Association and the Water Environment Federation, Washington DC.
28 P. L. Younger, *Q. J. Eng. Geol. Hydrogeol.*, 1995, **28**, S101–S113.
29 P. L. Younger, *J. Inst. Mining and Metal.*, 109, pp. A210–A218.
30 P. L. Younger, *J. Sci. Total Environ.*, 265, pp. 309–326.
31 P. L. Younger, *Appl. Geochem.*, 2000, **15**, 1383–1397.
32 P. L. Younger, *Sci. Total Environ.*, 2001, **265**, 309–326.
33 M. Hromadova and W. R. Fawcett, *J. Phys. Chem. A*, 2001, **105**, 104–111.
34 C. F. Baes and R. E. Mesmer, *The Hydrolysis of Cations*, Krieger, Florida pp 235-7.
35 C. F. Baes and R. E. Mesmer, *The Hydrolysis of Cations*, Krieger, Florida pp 226-8.
36 R. N. Sylva, *Pure. Appl. Chem.*, 1972, **22**, 115.
37 C. M. Flynn, *Chem. Rev.*, 1984, **84**, 31.
38 R. M. Cornell, R. Giovanoli and W. Schneider, *J. Chem. Tech. Biotechnol.*, 1989, **46**, 115.
39 W. Schneider, *Chimia*, 1988, **42**, 9.
40 W. Schneider and B. Schwyn, The hydrolysis of iron in synthetic, biological and aquatic media, in *Aquatic Surface Chemistry*, ed. W. Stumm., Wiley, New York, 1987, p 167.
41 G. Lente and I. Fábián, *Inorg. Chem.*, 1999, **38**, 603–605.
42 L. Lopes, J. de Laat and B. Legube, *Inorg. Chem.*, 2002, **41**, 2505–2517.
43 G. S. Pokrovskii, J. Schott, F. Farges and J.-L. Hazemann, *Geochim. Cosmochim. Acta*, 2003, **67**, 3559–3573.
44 D. T. Richens, *The chemistry of aqua ions: synthesis, structure and reactivity: a tour through the periodic table of the elements*. Wiley, New York, 1997 pp 372-376.
45 W. Feitknecht and W. Michaelis, *Helv. Chim. Acta*, 1962, **45**, 212.
46 O. Y. Pykhteev, A. A. Efimov and L. N. Moskvin, *Russ. J. Appl. Chem.*, 1999, **72**, 9–20.
47 B. A. Sommer and D. W. Margerum, *Inorg. Chem.*, 1970, **9**, 2517.
48 B. Lutz and H. Wendt, *Ber. Bunsenges. Phys. Chem.*, 1970, **74**, 372.
49 G. Biedermann and P. W. Schindler, *Acta Chem. Scand.*, 1957, **11**, 731.
50 A. P. Aldrich and C. M. G. van den Berg, *Electroanalysis*, 1998, **10**, 369–373.

